Proceedings of the 21st ICSMGE, Vienna, Austria, 14 – 19 June 2026. Pistrol, Adam & Schweiger (eds.)
Published by: ÖGG, Austrian Society for Geomechanics, Salzburg, Austria, ISBN 978-3-9503898-4-5
https://doi.org/10.53243/ICSMGE2026-696

Partially Drained Soil Behavior: Insights from Cyclic Tests

Jochen Zürn, Hans Henning Stutz
Institute of Soil Mechanics and Rock Mechanics, Karlsruhe Institute of Technology, Germany, Jochen.zuern@kit.edu

ABSTRACT: Geotechnical structures, foundations, and soils are subjected to cyclic loads such as earthquakes, waves, wind, or traffic loads. Traditionally, it is assumed that undrained conditions prevail during short-term loading events such as earthquakes, even in permeable soils like sand. This assumption is based on the premise that the drainage paths are too long relative to the loading duration for significant drainage to occur. However, recent research has shown that drainage occurs even during these conditions and must be considered. Partial drainage leads to simultaneous changes in pore water pressure and volumetric deformations, resulting in soil behaviour that differs from that under undrained conditions. This study investigates the effects of partial drainage conditions on the liquefaction resistance of sand by conducting cyclic, partially drained triaxial tests on Karlsruhe fine sand. The cyclic resistance ratio (CRR), derived from the test results, was used to quantify the liquefaction resistance. Several experimental methods from the literature were employed to induce partial drainage conditions. This enabled the analysis of these methods and their influence on the test results. Additionally, the test results were compared with those from undrained cyclic triaxial tests to evaluate the impact of partial drainage on the CRR. The findings reveal significant differences in CRR between undrained and partially drained conditions. This emphasizes that accounting for partial drainage is essential not only for more accurate estimations of in-situ soil behaviour but also for a better overall understanding of soil behaviour under cyclic loading. Neglecting it can lead to inaccuracies and uncertainties. Therefore, considering partial drainage will ultimately result in more efficient and reliable geotechnical designs.

KEYWORDS: Partial drainage, triaxial testing, cyclic loading, liquefaction resistance

1 INTRODUCTION

Geotechnical structures, soils, and foundations are frequently subjected to cyclic loading induced by wind, waves, earthquakes, or traffic. The soil response is traditionally classified as either drained or undrained depending on the magnitude, duration, and rate of loading. This classification is not only controlled by the load characteristics but also by factors such as drainage path length and soil permeability. Even for highly permeable soils such as sands, undrained behaviour is often assumed when assessing liquefaction resistance. This assumption is based on the premise that, for example during earthquakes, the loading duration is short and the drainage paths are long enough for drainage to be neglected.

In reality, in-situ conditions are not limited to fully drained or undrained states, where either volume change is inhibited (undrained) or pore water pressure remains constant (drained). Partially drained conditions frequently occur, characterised by simultaneous changes in pore water pressure u and volumetric strain ε_{vol}. Such conditions can arise, for example, in offshore foundations (e.g. Li et al. 2019; Jostad et al. 2022) and during earthquake loading (e.g. Lakeland et al. 2014; Adamidis & Madabhushi 2018).

Restricting the analysis of cyclic soil behaviour and liquefaction to fully undrained conditions therefore represents a simplification that can lead to inaccurate predictions of soil response and to over- or underestimation of liquefaction resistance. To improve the understanding of soil behaviour under partially drained conditions, experimental investigations that deliberately impose such drainage states are required. Various approaches to generate controlled partial drainage in laboratory tests have been proposed in the literature.

This study investigates several approaches to generate partially drained conditions in cyclic triaxial tests and evaluates their influence on soil behaviour and cyclic resistance ratio (CRR). Comparisons with conventional undrained tests provide insight into how the imposed drainage method influences the observed soil response.

2 PARTIALLY DRAINED TESTING METHODS

The following sections describes laboratory setup and procedures used to generate partially drained conditions in fully saturated specimens in a controlled manner.

Unsaturated specimens, which can also exhibit simultaneous changes of u and ε_{vol} are beyond the scope of this study. Similarly, centrifuge and model tests capable of reproducing partially drained conditions are likewise not considered here.

It is worth noting that even conventionally undrained triaxial tests are not perfectly isochoric. Small volumetric strains may occur due to membrane penetration and the compressibility of pore water and soil grains (Niemunis & Knittel 2020). For fine sands and within standard geotechnical stress ranges, these effects can be considered negligible. In the present work, tests conducted on Karlsruhe fine sand, described in detail later, fall into this category and are referred to as undrained (isochoric) for comparison purposes.

The following subsections summarise the laboratory techniques for imposing partially drained conditions that were investigated in this study.

2.1 *Increased drainage resistance*

Partially drained conditions can be generated by increasing the drainage resistance using a flow restrictor between the specimen and the volume measurement system. Common approaches include adjustable microvalves, highly impermeable filter plates installed in series, or a significant extension of the drainage path.

The permeability of the flow restrictor should be low compared to that of the tested soil so that the dissipation of the hydraulic head between the specimen and the volume measurement occurs almost entirely within the flow restrictor itself. Under these conditions, pore water pressure can be assumed to remain approximately homogeneous throughout the specimen during loading.

During cyclic loading, the pore water pressure within the specimen changes and dissipates slowly due to the imposed drainage resistance as water flows in or out of the specimen. Examples of cyclic triaxial tests on sands using this method can be found in Breth & Schwab (1977), Umehara et al. (1985), Jordan (1986) and Yamamoto et al. (2009).

The results of these studies demonstrated that the observed soil response depends on both the permeability k of the drainage element and the loading frequency f. The experiments show that liquefaction resistance increases with decreasing loading frequency and with decreased drainage resistance. A

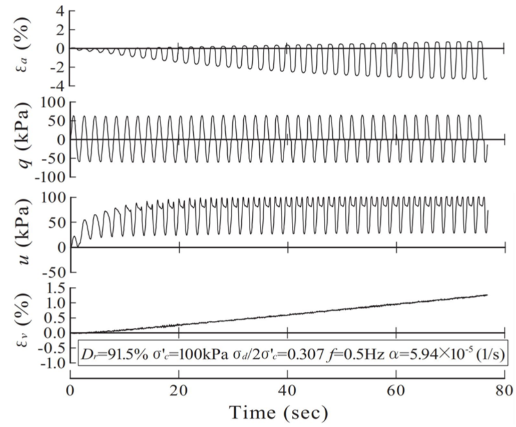

Figure 1. Typical results of cyclic partially drained triaxial tests with increased drainage resistance, showing the time histories of ε_a, q, u, and ε_{vol} (Yamamoto et al. 2009)

threshold combination of k, f and cyclic loading was identified beyond which liquefaction no longer occurs: in this regime, the accumulation of excess pore water pressure is slower than its dissipation through drainage, leading to a recovery of mean effective stress p after initial relaxation.

Figure 1 shows a typical test result with increased drainage resistance, illustrating the pore pressure build-up and ε_{vol} over time.

In contrast to cyclic loading, monotonic triaxial tests with increased drainage resistance have been conducted only rarely. Suzuki et al. (2020) performed such tests and reported results that fell between those of fully drained and fully undrained reference tests. Similar to the cyclic experiments, the monotonic results demonstrated a clear dependence on both the imposed drainage resistance and the applied loading rate.

2.2 *Imposed strain path*

Another widely used approach to generate and investigate partially drained conditions in the laboratory is the imposition of a prescribed strain path. This method has been applied primarily in monotonic triaxial tests, with particular focus on linear strain paths (e.g. Vaid & Eliadorani 1998; Eliadorani 2000; Sivathayalan & Logeswaran 2007; Jrad et al. 2012; Adamidis et al. 2018). Different constant ratios of volumetric to axial strain, $\zeta = \dot{\varepsilon}_{vol}/\dot{\varepsilon}_a$, are imposed by actively injecting or extracting water from the specimen and controlling ε_a. Both expansive ($\zeta < 0$) and contractive ($\zeta > 0$) strain paths have been studied. A value of $\zeta = 0$ corresponds to a conventional undrained test with $\dot{\varepsilon}_{vol} = 0$.

The measured stress–strain behaviour is highly dependent on the imposed strain path. Expansive paths typically lead to a reduction in p and lower maximum achievable deviatoric stresses q, while even small amounts of water outflow during contractive paths can cause an increase in p and maximum q. Non-linear strain paths have also been investigated (e.g. Sivathayalan & Logeswaran 2008), with the stress response again showing a strong sensitivity to the imposed volumetric–axial strain relationship. It should be noted that monotonic tests under imposed strain paths can produce results outside the fully drained and undrained reference curves.

Adamidis & Anastasopoulos (2024) extended this concept to cyclic triaxial testing by applying a constant water inflow into the specimen during cyclic loading using a volume–pressure controller. Such water inflows can also occur in-situ during earthquakes, particularly in layered deposits with contrasting permeabilities. As demonstrated by Cubrinovski et al. (2019) and Tsaparli et al. (2020), such drainage effects can significantly influence liquefaction susceptibility and may lead to erroneous assessments of liquefaction resistance if ignored.

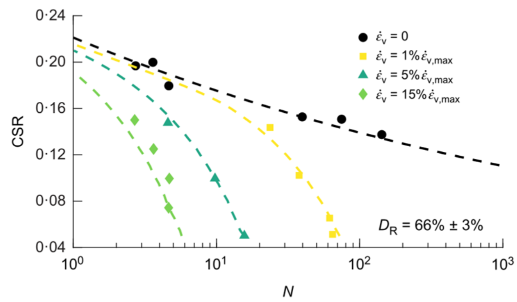

Figure 2. Number of cycles to onset of liquefaction for different imposed inflow rates and cyclic stress ratios (Adamidis & Anastasopoulos 2024)

In their experiments, Adamidis & Anastasopoulos (2024) aimed to select inflow rates within a realistic range. The number of cycles to the onset of liquefaction for different inflow rates and cyclic stress ratios ($\mathrm{CSR} = q^{\mathrm{ampl}}/2p_0$) is presented in Figure 2. The results show a marked reduction in the number of cycles required to reach liquefaction compared to undrained reference tests, with the effect being more pronounced for higher volumetric strain rates $\dot{\varepsilon}_{vol}$. It was further demonstrated that the cyclic resistance for a given water inflow can be reasonably estimated using the undrained cyclic resistance curve in combination with the isotropic unloading line (dotted lines in Figure 2).

2.3 *Adjustment of Fluid Bulk Modulus K_f*

A further method for partially drained tests was recently introduced by Zuern et al. (2024). A schematic of the experimental setup is shown in Figure 3. In this approach, an enclosed gas bubble is incorporated into the test setup, resulting in a direct coupling between the volumetric strain rate $\dot{\varepsilon}_{vol}$ and the rate of pore water pressure change $\dot{u}$.

The initial gas bubble volume $V_{a,0}$ and gas pressure $u_{a,0}$ can be freely adjusted prior to the test. Any volumetric change in the specimen during the test causes compression or expansion of the gas bubble, accompanied by a corresponding change in gas pressure u_a according to Boyle-Mariotte law $u_a^{tot} \cdot V_a = \mathrm{const}$, where u_a^{tot} is the absolute gas pressure including atmospheric pressure. This change in gas pressure affects the pore water, thereby changing the pore water pressure. By selecting $V_{a,0}$ and $u_{a,0}$, the bulk modulus of the pore fluid system K_f can be controlled, allowing the test conditions to be tuned between fully drained ($K_f \to 0$) and undrained ($K_f \to K_w$), where $K_w = 2.2$ GPa is the bulk modulus of water.

Monotonic tests using this method showed a rate-independent and specimen-size-independent soil response between drained and undrained reference tests. Increasing the initial bulk modulus $K_{f,0}$, achieved by reducing the chosen initial gas volumes $V_{a,0}$ or increasing $u_{a,0}$, resulted in a more undrained soil response.

In contrast to the increased drainage resistance and imposed strain path methods, this approach enables the investigation of partially drained behaviour without introducing rate effects or prescribing a specific strain path. Cyclic triaxial tests using this method have not yet been reported in the literature, and the present work represents the first attempt to investigate partially drained cyclic behaviour with this approach.

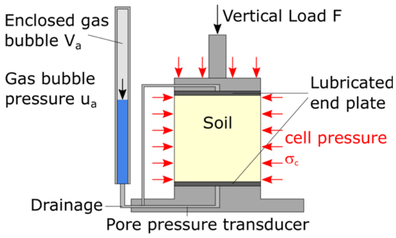

Figure 3. Schematic experimental setup for generating partially drained conditions through adjustment of the pore fluid bulk modulus K_{f} (Zuern et al. 2024)

2.4 *Additional methods not investigated*

In fine-grained soils subjected to rapid loading, the rate of loading may exceed the rate of pore pressure equalisation within the specimen. Laboratory studies have used such conditions to investigate partially drained behaviour in low-permeability soils. The resulting response involves simultaneous changes of u and $\varepsilon_{\mathrm{vol}}$ that are not homogeneously distributed throughout the specimen. Similar effects could also occur in sands under very rapid loading.

Another laboratory technique employed to study partially drained behaviour is intermittent drainage, in which a certain amount of water is allowed to drain after a number of undrained cycles before resuming cyclic loading under undrained conditions (e.g. Lee and Focht 1975; Schuppener 1981). The amount of water released is often estimated based on consolidation theory.

3 TEST MATERIAL

All experiments in this study were carried out on Karlsruhe fine sand (KFS), a uniformly graded, fine quartz sand that has been extensively characterised in previous research (e.g. Wichtmann 2016; Zuern et al. 2024; Mugele et al. 2025). The grain size distribution is shown in Figure 4, and the key index properties of the material are summarised in Table 1.

4 TEST METHODS AND CONDITIONS

All tests were performed on cylindrical specimens prepared by dry air pluviation to a target relative density of approximately $I_{\mathrm{d,0}} = \frac{e_{\mathrm{m}}-e}{e_{\max}-e_{\min}} \approx 0.60$. The specimens had a diameter and height of 100 mm. Lubricated end platens were used to minimise end friction effects. All tests were conducted from an identical isotropic initial state of $p = 200$ kPa, followed by the application of a cyclic deviatoric stress. Three different approaches to impose partially drained conditions were employed: (i) increased drainage resistance, (ii) constant imposed inflow rate, and (iii) adjustment of K_{f}. For reference, undrained cyclic triaxial tests on KFS performed by Wichtmann & Triantafyllidis (2016) were used. These reference tests were carried out out in the same laboratory using material from the same batch, ensuring minimal influence from specimen preparation or material variability and allowing for direct comparison. An overview of all tests is given in Table 2.

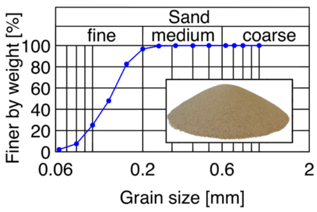

Figure 4. Grain size distribution of Karlsruhe fine sand (KFS)

Table 1. Characteristic values of KFS (Wichtmann 2016)

d_{50} [mm]	C_u [-]	ρ_s [g/cm^3]	e_{min} [-]	e_{max} [-]
0.14	1.5	2.65	0.677	1.054

4.1 *Increases drainage resistance*

Tests with increased drainage resistance (TCDR_ series) were carried out in a stress-controlled triaxial apparatus. Partial drainage was induced by inserting a highly impermeable porous stone between the specimen and the volume change measurement device. The permeability of the porous stone was calibrated by measuring flow rates under different pressure differentials in the relevant stress range. The results showed a linear relationship between flow and pressure difference, indicating laminar flow conditions. Post-test evaluations using measured pore pressures and volume changes confirmed that the drainage resistance remained constant throughout the experiments. Within this series, the cyclic loading frequency f and the deviatoric stress amplitude q^{ampl} were varied systematically.

4.2 *Constant imposed inflow rate*

Tests with a constant imposed water inflow or outflow (TCIn and TCOut series) were conducted in a stress-controlled triaxial apparatus. A volume–pressure controller was used to apply a constant water flow rate during cyclic loading. The flow rate was selected to achieve a target volumetric strain change per cycle. q^{ampl}, the direction of water flow (inflow vs. outflow) and target volumetric strain change per cycle were varied between tests.

4.3 *Adjustment of pore fluid bulk modulus K_f*

Tests with adjusted K_{f} (TCKf series) were conducted in a displacement-controlled triaxial device. Cyclic loading was applied using a constant axial displacement rate of 0.05 mm/min. A pseudo-stress-control procedure was implemented by reversing the loading direction whenever the current q crossed the predefined deviatoric stress limits. All tests were conducted with an initial effective pore fluid bulk modulus of approximately $K_{\mathrm{f,0}} \approx 33$ MPa. q^{ampl} was varied between tests.

The undrained reference tests by Wichtmann & Triantafyllidis (2016) employed the same pseudo-stress-control procedure and identical axial displacement rates.

4.4 *Definition of onset of liquefaction behaviour*

In this study, the onset of liquefaction behaviour was determined using the crossing of the phase transformation line (PTL) as a criterion. The PTL slopes in compression and extension were taken from Wichtmann (2016) for a relative density of $I_{\mathrm{d,0}} = 0.60$. For medium-dense sand, previous studies have shown that the number of cycles to reach the PTL or to reach an axial strain amplitude of approximately 5 % are comparable for both partially drained and undrained conditions (Yamamoto et al 2009; Adamidis & Anastasopoulos 2024).

The commonly used $p = 0$ criterion was not applied to maintain a consistent definition across all tests. In some of the stress-controlled experiments, the axial displacement rate exceeded a defined limit before p approached zero due to specimen softening. This limit was set to 1.0 mm/min to ensure quasi-static conditions in the tests. The displacement rate was computed as $\dot{s} = \Delta s / \Delta t$ using a time interval corresponding to 10 % of the cycle duration.

Table 2 includes the number of cycles N required to cross the PTL for all tests. It should be noted that, for the undrained Reference tests, the number of cycles to cross the PTL was obtained by re-evaluating the original data from Wichtmann &

Table 2. Overview of the experiments on KFS

Test	I_{D0} [-]	q^{ampl} [kPa]	f [Hz]	$\dot{\varepsilon}_{vol}$ [%/Cycle]	N [-]
TCDR1	0.64	60	0.01		11
TCDR2	0.66	40	0.01		-
TCDR3	0.62	50	0.01		17
TCDR4	0.64	50	0.0005		-
TCIn1	0.63	10	0.001	0.01	48
TCIn2	0.64	20	0.001	0.01	36
TCIn3	0.62	40	0.001	0.01	17
TCIn4	0.65	10	0.00005	0.1	6
TCOut1	0.64	10	0.001	-0.01	-
TCKf1	0.58	60			272
TCKf2	0.61	70			72
TCKf3	0.58	75			34
TCUI7*	0.67	60			10
TCUI11*	0.56	40			145
TCUI12*	0.64	50			76
TCUI13*	0.59	60			14

* Wichtmann & Triantafyllidis (2016)

Triantafyllidis (2016) using the PTL criterion. As a result, these values are marginally lower than the numbers reported for initial liquefaction in the original publication. This further confirms that the use of the PTL criterion does not significantly affect the resulting cycle counts. It should also be noted that the undrained reference tests (TCUI11, TCUI12, TCUI13) were conducted with a drained first loading cycle. This initial drained preloading is known to slightly reduce the initial stress relaxation rate, resulting in slightly higher cycle numbers for liquefaction (Wichtmann & Triantafyllidis 2016).

5 TEST RESULTS

All tests conducted in this study successfully showed partially drained conditions, as indicated by the simultaneous development of pore water pressure u and volumetric strain ε_{vol} during cyclic loading. Test data were evaluated until either an axial strain of 10 % or an axial displacement rate of 1 mm/min, whichever occurred first.

The following subsections first presents the characteristic behaviour observed for each testing method. Afterwards, the influence of the different methods on liquefaction resistance is compared.

5.1 *Increases drainage resistance*

All tests with increased drainage resistance showed densification under cyclic loading. The stress path exhibited progressive relaxation of p accompanied by an increase in u. Figure 5 shows the stress path and volumetric strain over time for test TCDR1. Due to the increased drainage resistance, pore pressure dissipation lagged behind the cyclically induced build-up of u. The resulting water outflow caused a reduction in specimen volume, with the volumetric strain rate being directly governed by the excess pore water pressure. At the beginning of the tests, when u was still low, the volumetric strain rate remained small; as u increased during loading, the rate of volumetric contraction accelerated correspondingly. The characteristic butterfly-shaped stress loops typically observed after liquefaction were not captured in this case because the test

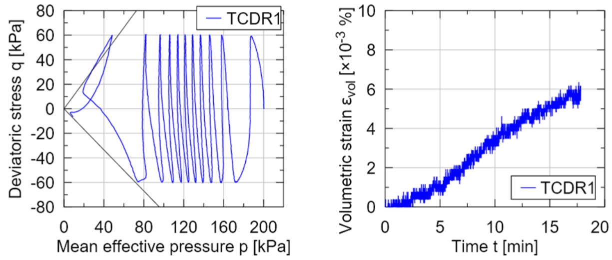

Figure 5. Cyclic triaxial test with increased drainage resistance. Left: Stress path in t he $p-q$ diagram. Right: Evolution of ε_{vol} over time

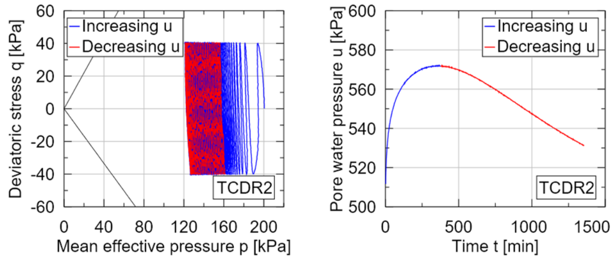

Figure 6. Cyclic triaxial test with increased drainage resistance. Left: Stress path in the $p-q$ diagram. Right: Trend of u over time

was terminated when the axial displacement rate exceeded the 1 mm/min evaluation limit.

In contrast to TCDR1 and TCDR3, tests TCDR2 and TCDR4 did not reach liquefaction. TCDR2, performed at the same frequency as TCDR1 and TCDR3 but at a lower q^{ampl}, initially exhibited a relaxation of p with a concurrent increase in u, followed by a reversal. p increased again while u decreased as drainage outpaced pore water pressure accumulation. The corresponding stress path and trend of the pore water pressure over time for TCDR2 are presented in Figure 6.

Test TCDR4, conducted at the same $q^{ampl} = 50$ kPa as TCDR3 but at 1/20th of the frequency, showed a similar behaviour. In TCDR4, the maximum pore water pressure was reached after only four cycles before dissipation became dominated. In comparison, TCDR3 crossed the PTL after 17 cycles. These results highlight the strong time-dependence of the increased drainage resistance method and indicate a threshold combination of stress amplitude and frequency beyond which liquefaction does not occur.

5.2 *Constant imposed inflow rate (TCIn/TCOut)*

Tests with constant imposed water inflow (TCIn series) were the only tests that exhibited a net increase in specimen volume during cyclic loading. All specimens in this series liquefied significantly faster than those in the undrained reference tests. For example, specimen TCIn1 crossed the PTL after only 17 cycles at $q^{ampl} = 40$ kPa, compared to 145 cycles in the undrained test TCUI11. The relative density changed only slightly (I_D: 0.62 → 0.61), indicating that isotropic unloading from water inflow dominated the relaxation of p rather than the cyclic loading, even for such small volume changes. Figure 7 shows the stress path and ε_{vol} over time for test TCIn3 as a representative example.

A second test with the same $q^{ampl} = 10$ kPa but a tenfold higher volumetric strain increment per cycle crossed the PTL after only six cycles, compared to 48 cycles in the lower-rate test. The relative density change was again minimal (I_D: 0.65 → 0.64). This pronounced difference highlights the high sensitivity of cyclic resistance to the imposed volumetric strain rate during loading. Even an initially looser specimen would not have resulted in such a pronounced reduction in the number of cycles as observed with the imposed water inflow.

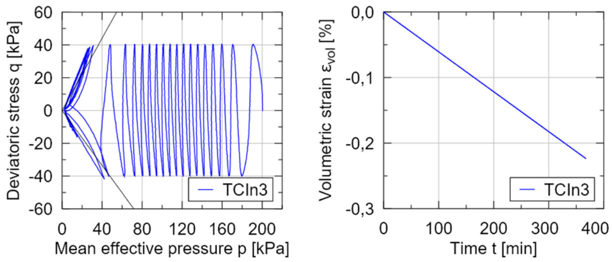

Figure 7. Cyclic triaxial test with constant inflow rate. Left: Stress path in the $p - q$ diagram. Right: Evolution of $\varepsilon_{\mathrm{vol}}$ over time

In contrast, the TCOut1 test with constant water outflow produced progressive densification and a marked increase in cyclic resistance. While TCIn1 showed a monotonic relaxation of p until liquefaction, TCOut1 exhibited an immediate rise in p and a reduction in u and and no tendency towards liquefaction was observed.

These findings demonstrate that even very small water flow during cyclic loading can dramatically alter liquefaction resistance, with the direction of flow (inflow versus outflow) controlling whether the soil response weakens or strengthens.

5.3 *Adjusted pore fluid bulk modulus K_f (TCKf)*

The TCKf series showed densification under cyclic loading. This led to a water outflow out of the specimen and compression of the enclosed gas bubble, thereby increasing gas pressure. The stress path exhibited progressive relaxation of p accompanied by an increase in u. The stress path and volumetric strain over time for test TCKf3 is shown in Figure 8. Excess pore water pressure build-up showed, as well as $\varepsilon_{\mathrm{vol}}$ the charactersistic S-shaped accumulation over time, that can be also observed in the undrained reference tests. All tests liquified an showed the typical butterfly-shaped effective stress loops after liquefaction. After liquefaction also dilatant phases with an increase of specimen volume can be observed after longer phases with no to little change of $\varepsilon_{\mathrm{vol}}$. This dilatant phases are accompanied by increases of $|q|$. This experiment clearly shows that the increases of $|q|$ after long shearing in the liquefied state (cyclic mobility) are accompanied by dilatancy behaviour of the specimen. For undrained experiments, in which there is no volume deformation, this is explained by prevented dilatancy, which is indicated by a decrease of excess pore water pressure. In these partially drained experiments, this dilatancy behaviour can be observed directly.

It should be noted that during the tests some dissolution and diffusion of gas into the pore water may occur, and this process is inherently time-dependent. Zuern et al. (2024) demonstrated for monotonic triaxial tests with durations between 5 h and 50 h that this effect is negligible within that range. In the present study, the longest test duration until crossing the PTL was 37 h (test TCKf1), suggesting that the influence of gas dissolution and diffusion on the measured number of cycles is minor. Nevertheless, this aspect should be verified in future work by conducting comparative tests with different overall durations.

5.4 *Liquefaction resistance and comparison of the testing methods*

Figure 9 shows the number of cycles N to the first crossing of the phase transformation line (PTL) plotted against the CSR for all tests. Such diagrams are commonly used to derive the cyclic resistance ratio (CRR), a key parameter for characterizing liquefaction resistance. Dashed lines indicate trendlines for test series in which only the cyclic stress amplitude q^{ampl} and thus

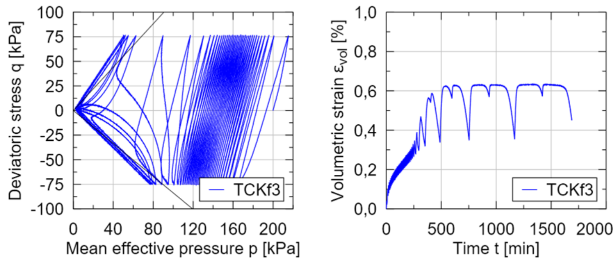

Figure 8. Cyclic triaxial test with adjusted K_f. Left: Stress path in the $p - q$ diagram. Right: Evolution of $\varepsilon_{\mathrm{vol}}$ over time

CSR were varied. The results reveal a clear influence of the testing method and the imposed partially drained conditions on liquefaction resistance, which is summarised below:

- **Increased drainage resistance:** Tests with increased drainage resistance showed an increase in liquefaction resistance compared to the undrained reference tests. This increase is small at higher CSR but becomes more pronounced as CSR decreases, ultimately resulting in test conditions where liquefaction does not occur. Tests that did not reach liquefaction are shown as open symbols, placed at the cycle number corresponding to the maximum observed pore water pressure. From these non-liquefied tests, a threshold can be identified that marks the limit beyond which liquefaction is not observed. The position of the threshold is not constant but depends on both the magnitude of the drainage resistance and the applied loading frequency.
- **Adjustment of K_{f}:** Reducing the initial pore fluid bulk modulus to approximately $K_{\mathrm{f,0}} \approx 33$ MPa significantly increased liquefaction resistance. No distinct threshold CSR was identified beyond which liquefaction was prevented. Higher $K_{\mathrm{f,0}}$ values would be expected to shift the response closer to undrained behaviour, accompanied by a corresponding decrease in CRR.
- **Constant imposed inflow rate:** In contrast, tests with imposed water inflow exhibited a strong reduction in liquefaction resistance compared to the undrained reference tests. In extreme cases (e.g. TCIn4), the specimens showed only very low resistance to liquefaction. Furthermore, the typical trend of sharply increasing N with decreasing CSR was inverted: reducing CSR resulted in only a marginal increase in the number of cycles to the onset of liquefaction. This behaviour is attributed to the constant water inflow, which caused continuous isotropic unloading throughout the test.

The results demonstrate that partially drained conditions can substantially alter CRR compared to undrained behaviour. The derived liquefaction resistances and their trends are highly sensitive to the specific method used to impose partial drainage, underlining the crucial role of boundary conditions in cyclic testing. Crucial are the direction and magnitude of water flow and the associated change of volumetric strain. Even small amounts of inflow or outflow can drastically change liquefaction resistance, despite causing only minor changes in void ratio or relative density.

Assuming fully undrained behaviour, as is standard in many liquefaction assessments, may therefore lead to significant over- or underestimation of liquefaction resistance when partially drained conditions are present. Practical recommendations for engineering practice cannot yet be drawn, as the present study is based solely on medium-dense specimens of a single material.

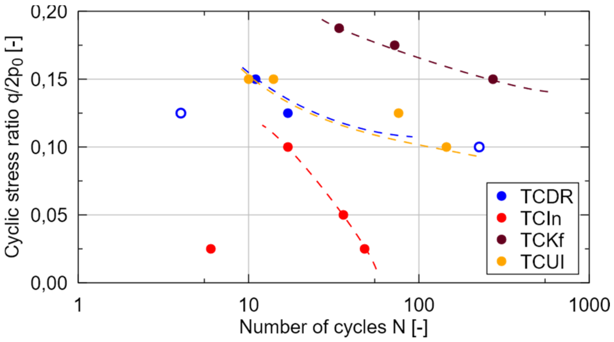

Figure 9. Cyclic stress ratio (CSR) plotted against the number of cycles to first crossing of the phase transformation line (PTL). Dashed lines: Trendlines derived from test series differing only in CSR. Open symbols: Number of cycles at which the maximum pore water pressure was reached in non-liquefied tests

6 CONCLUSIONS

This study investigated the influence of partially drained conditions on liquefaction resistance in cyclic triaxial tests. Three methods discussed in the literature were employed to impose partial drainage: (i) increasing drainage resistance, (ii) applying a constant water inflow or outflow during cyclic loading, and (iii) adjusting the pore fluid bulk modulus K_f using an enclosed gas bubble.

Across all methods, simultaneous changes in pore water pressure u and volumetric strain ε_{vol} were observed, confirming the generation of partially drained conditions. Comparison with undrained reference tests demonstrated that the chosen testing method has a strong effect on the liquefaction resistance. This underlines that “partially drained” is not a single, clearly defined state but a range of conditions whose interpretation depends on the specific boundary conditions imposed in the laboratory.

A key finding is the dominant role of volumetric strain changes on soil response: even very small inflows or outflows of water, resulting in minor changes of ε_{vol} can dramatically increase or reduce CRR, in some cases preventing liquefaction entirely or almost eliminating resistance. Consequently, assuming fully undrained behaviour, as is common in liquefaction assessments, can lead to significant over- or underestimation of liquefaction resistance when partially drained conditions are present. Accounting for partial drainage and changes of ε_{vol} in the evaluation of soil behaviour is essential for improving predictions of liquefaction resistance and for enabling safe and efficient design practice.

7 REFERENCES

Adamidis, O. and Madabhushi, S.P.G., 2018. Experimental investigation of drainage during earthquake-induced liquefaction. *Géotechnique*, 68(8), pp.655-665. https://doi.org/10.1680/jgeot.16.P.090

Adamidis, O. and Anastasopoulos, I., 2024. Cyclic liquefaction resistance of sand under a constant inflow rate. *Géotechnique*, 74(10), pp.1019-1032. https://doi.org/10.1680/jgeot.21.00082

Breth, H. and Schwab, H., 1977. Liquefaction of a fully saturated sand under anisotropic initial states of stress in a controlled drainage system. *Proc. of DMSR 77*, vol.2., pp.149-159

Cubrinovski, M., Rhodes, A., Ntritsos, N. and Van Ballegooy, S., 2019. System response of liquefiable deposits. *Soil Dynamics and Earthquake Engineering*, 124, pp.212–229. https://doi.org/10.1016/j.soildyn.2018.05.013.

Eliadorani, A., 2000. *The response of sands under partially drained states with emphasis on liquefaction*. Ph.D. thesis. University of British Columbia, Canada.

Jrad, M., Sukumaran, B. and Daouadji, A., 2012. Experimental analyses of the behaviour of saturated granular materials during axisymmetric proportional strain paths. *European Journal of Environmental and Civil Engineering*, 16(1), pp.111–120. https://doi.org/10.1080/19648189.2012.666900.

Jordan, P., 1986. *Einfluss der Belastungsfrequenz und der partiellen Entwässerungsmöglichkeiten auf die Verflüssigung von Feinsand*. Ph.D. thesis. Ruhr-Universität Bochum.

Jostad, H. P., Liu, H., Sivasithamparam, N. and Ragni, R., 2022. Cyclic capacity of monopiles in sand under partially drained conditions: A numerical approach. *Journal of Geotechnical and Geoenvironmental Engineering*, 149(2). https://doi.org/10.1061/JGGEFK.GTENG-10435

Lakeland, D.L., Rechenmacher, A. and Ghanem, R., 2014. Towards a complete model of soil liquefaction: the importance of fluid flow and grain motion. *Proceedings of the Royal Society A: Mathematical, Physical and Engineering Sciences*, 470(2165). http://dx.doi.org/10.1098/rspa.2013.0453

Lee, K. L. and Focht, J. A., 1975. Liquefaction potential at the Ekofisk Tank in the North Sea. *Journal of the Geotechnical Engineering Division,* 100(GT1).

Li, S., Zhang, Y. and Jostad, H.P., 2019. Drainage conditions around monopiles in sand. *Applied Ocean Research*, 86, pp.111-116. https://doi.org/10.1016/j.apor.2019.01.024

Mugele, L., Zürn, J., Niemunis, A. and Stutz, H. H., 2025. Experimental study of the soil structure variable z used in constitutive models such as Neohypoplasticity or Sanisand. *IOP Conference Series: Earth and Environmental Science*, 1480, Article no. 012070. https://doi.org/10.1088/1755-1315/1480/1/012070

Niemunis, A. and Knittel, L., 2020. Removal of the membrane penetration error from triaxial data. *Open Geotechnics*, 2, Article no. 5. https://doi.org/10.5802/ogeo.7

Sivathayalan, S. and Logeswaran, P., 2007. Behaviour of sands under generalized drainage boundary conditions. *Canadian Geotechnical Journal*, 44(2). https://doi.org/10.1139/t06-110

Sivathayalan, S. and Logeswaran, P., 2008. Experimental assessment of the response of sands under shear-volume coupled deformation. *Canadian Geotechnical Journal*, 45(9). https://doi.org/10.1139/T08-068

Schuppener, B., 1981. *Porenwasserdruck im Sand unter Wellenbelastung auf Offshore-Bauwerken*. Ph.D. thesis. Technische Universität Braunschweig.

Suzuki, Y., Carotenuto, P., Dyvik, R. and Jostad, H.P., 2020. Experimental study of modelling partially drained dense sand behaviour in monotonic triaxial compression loading tests. *Geotechnical Testing Journal*, 43(5). https://doi.org/10.1520/GTJ20190097

Tsaparli, V., Kontoe, S., Taborda, D.M. and Potts, D.M., 2020. A case study of liquefaction: demonstrating the application of an advanced model and understanding the pitfalls of the simplified procedure. *Géotechnique*, 70(6), pp.538–558. https://doi.org/10.1680/jgeot.18.P.263.

Umehara, Y., Zen, K. and Hamada, K., 1985. Evaluation of soils liquefaction potentials in partially drained conditions. *Soils and Foundations*, 25(2), pp.57-72. https://doi.org/10.3208/sandf1972.25.2_57

Vaid, Y.P. and Eliadorani, A., 1998. Instability and liquefaction of granular soils under undrained and partially drained states. *Canadian Geotechnical Journal*, 35(6). https://doi.org/10.1139/t98-061

Wichtmann, T., 2016. *Soil behaviour under cyclic loading – experimental observations, constitutive description and applications*. Habilitation. Karlsruher Institut für Technologie, vol.181.

Wichtmann, T. and Triantafyllidis, T., 2016. An experimental database for the development, calibration and verification of constitutive models for sand with focus on cyclic loading: Part I—tests with monotonic loading and stress cycles. *Acta Geotechnica*, 11, pp.739-761. https://doi.org/10.1007/s11440-015-0402-z

Yamamoto, Y., Hyodo, M. and Orsense, R.P., 2009. Liquefaction resistance of sandy soils under partially drained conditions. *Journal of Geotechnical and Geoenvironmental Engineering*, 135(8). https://doi.org/10.1061/(ASCE)GT.1943-5606.0000051

Zürn, J., Mugele, L. and Stutz, H.H., 2024. Novel experimental method for rate-independent triaxial tests under partial drainage condition. *Geotechnique Letters*, 14(3), pp.100–105. https://doi.org/10.1680/jgele.23.00120